3D PRINTED LAYER OF POLYANILINE-BASED CONDUCTIVE POLYMER FOR LIGHTNING STRIKE PROTECTION OF CFRPS

Vipin Kumar[1*], Ryan Spencer[2], Justin C. Condon[1], Tyler Smith[1], Tomohiro Yokozeki[3], Ahmed A. Hassen[1], Uday Vaidya[1,2], Vlastimil Kunc[1]

[1] Material Sciences and Technology Division, Manufacturing Demonstration Facility (MDF), Oak Ridge National Laboratory (ORNL), 2350 Cherahala Blvd, Knoxville, TN 37932, USA
[2]Department of Mechanical, Aerospace and Biomedical Engineering, University of Tennessee, Middle Drive, Knoxville, TN 37996, USA
[3] Department of Aeronautics and Astronautics, The University of Tokyo, Hongo Bunkyo-Ku, Tokyo 113-8654, Japan

*kumarvi@ornl.gov

ABSTRACT

Manufacturing of Carbon Fiber Reinforced Plastics (CFRPs) using additive manufacturing (AM), or 3D printing, has gained popularity in recent years. It is believed that the AM industry has the potential to manufacture CFRP parts in a faster, easier and more economical way. Lightning strike damage to CFRP parts is not rare; therefore, additional lightning strike protection (LSP) technologies are applied on top of CFRP structures. However, there is no report of manufacturing lightning strike protection (LSP) technologies using the AM process. In the present work, the authors applied an electrically conductive layer via additive manufacturing. The material of the electrically conductive layer was a Polyaniline (PANI)-filled thermoset composite. This layer of PANI was deposited on top of the CFRP panels. The PANI-coated CFRP panels were tested against a simulated lightning strike made of a continuous waveform with component A (100 kA), component B (2 kA) and component C (470 A). The highly conductive PANI-layer worked as a capable Faraday cage to safely dissipate the lightning current. In PANI-based LSP, direct contact between PANI chains dominated the conduction behavior, which proved to be a highly efficient way to reduce resistive heating from the incident current. However, poor adhesion between the printed layer and the substrate structure needs to be improved in the future. The results from the thermal camera and the high-speed camera images showed an effective current dissipation through the printed layers. Non-destructive ultrasonic imaging was done to confirm the direct lightning damages to samples. The present work shows that a non-metallic conductive layer can be applied as an LSP of CFRP structures via an additive manufacturing technique.

ACRONYMS AND SYMBOLS

CFRP, Carbon fiber reinforced plastic; FRP, Fiber reinforced plastic; LSP, Lightning strike Protection; FRP, Fiber reinforced polymer; EMF, Expanded metal foil; CNF, Carbon nanofiber; PANI, Polyaniline; DBSA, Dodecyl benzenesulfonic acid; CF, Carbon Fiber; DVB, Divinylbenzene;

INTRODUCTION

Additive Manufacturing (AM) of polymer composites with or without carbon fiber filler is already attracting much attention from researchers around the globe [1,2]. With the increasing interest in the large-scale production of continuous Carbon Fiber Reinforced Plastic (CFRP) using Big Area Additive Manufacturing (BAAM), AM is on a path towards solving a long-standing issue associated with AM: mass manufacturing [3]. Many industries are looking to commercialize the 3D printed CFRPs for actual structural applications. 3D printed metal-based components are already being used in some practical applications [4].

However, there are still some challenges, such as porosity, bad interphase, low Z-direction strength, and poor surface finish of the printed parts, which make AM inferior to the already commercially available CFRP manufacturing techniques [5]. The direction of a lot of the ongoing research is to overcome these challenges and produce CFRP structures via AM processes [6]. CFRPs are mainly used in aircrafts, wind turbines, and automobiles.

Among them, aircrafts and wind turbines are particularly at risk of lightning strikes due to their operating locations [7]. The low electrical conductivity of a CFRP structure makes them vulnerable to lightning strikes and, therefore, they need to be protected with the use of metal-based electrically conductive meshes or foils. These electrically conductive protections help safely dissipatation of lightning currents. However, recently, these well-known metal-based LSPs are being challenged by conductive non-metal or polymer-based LSPs [8,9]. Even so, there is no report on the use of non-metallic LSPs in actual applications.

Kumar et al., Katunin et al. and Hirano et al. have done a lot of work to establish Polyaniline (an intrinsically conductive polymer) as a potential LSP material [10–12]. Initially, they utilized a PANI-based resin to prepare electrically conductive CFRPs (CF/PANI). However, they reported deficient mechanical properties of the CF/PANI compared to the traditional epoxy-based CFRPs (CF/Epoxy). The low mechanical properties of CF/PANI limit its usage in practical applications where load bearing is the primary role of CFRP structures. In another attempt by researchers, a modified way of using a PANI-layer with CFRP was reported; they prepared a separate conductive layer of PANI and attached it to the substrate CF/Epoxy structure, as shown in Figure 1 [9]. They showed that this PANI-layer was a highly effective LSP that did not compromise the mechanical strength of the CFRP.

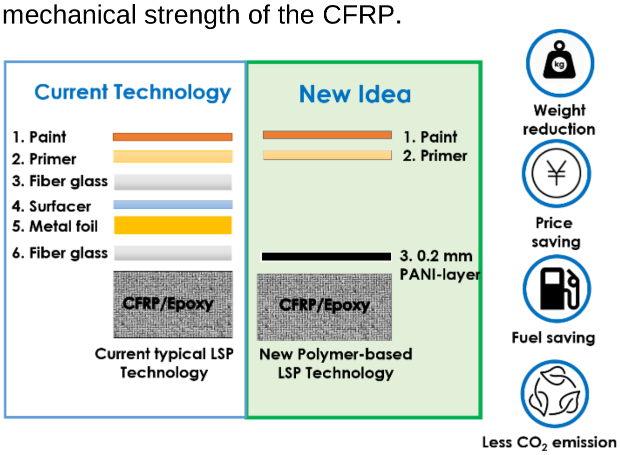

Figure 1. Concept of all-polymeric lightning strike protection material for CFRPs.

In the present work, AM is utilized to deposit a similar composition of an electrically conductive PANI-based polymer on top of a CFRP substrate. The viscosity of the resin was modified to suit the need of a 3D printer. 3D printed LSP with 3D printed continuous carbon fiber composite has the potential to minimize the associated cost with LSP integration.

EXPERIMENTAL DESIGN

Materials

Polyaniline in its emeraldine base form was procured from Kaken Sangyo Co. Ltd (Japan). Dodecyl benzenesulfonic acid (DBSA), divinylbenzene (DVB), hydroxybenzene sulfonic acid were purchased from Sigma Aldrich (USA). Kayahard GPH-65 Phenolic hardener was obtained from Nipponkayaku Co. Ltd (Japan).

PANI and DBSA were mixed in a 1:2.5 wt. ratio and provided with thermal treatment to obtain a controlled semi-doped complex of PANI-DBSA [13]. Meanwhile, DVB and a phenol hardener were also mixed using a centrifugal mixer in a 7:3 wt.% ratio. Furthermore, these Phenol-DVB and PANI-DBSA complexes were mixed using a mortar-pestle and a centrifugal mixer to obtain a final homogenous printable resin. The viscosity of the resin was controlled by adding 10 wt. % of hydroxybenzene sulfonic acid during mixing. The final material was used for printing an electrically conductive polymer layer on a CFRP structure.

CFRP panels were prepared using prepreg from Raptor Resin (USA). Carbon Fiber T300-12 K (2×22 twill weave) and BMI-1-OOA resin were the constituents of the prepreg. The prepreg fabric was cut into 20 cm × 20 cm sheets, and an 8-layer laminate was prepared using hot-press curing. The thickness of the obtained panels was around 2.35 (0.07) mm. An unprotected CFRP panel was painted with a dielectric paint and tested as a base material. Prepared samples and their parameters are shown in Table 1. In one sample, the thickness of the printed layer was intentionally increased by around half of the thickness of the CF/BMI-PD sample to study the effect of the thickness of the printed layer on the damage done by a lightning strike.

Table 1. Prepared samples and their properties.

Sample name	Printed Layer	Layer conductivity (S/cm)	Layer thickness (mm)
CF/BMI-PDD	PANI-DBSA/ DVB	0.91	1.23
CF/BMI-PD	PANI-DBSA	15.01	0.61/1.35
CF/BMI-Paint	Dielectric Paint	-	0.05

3D printing

Hydra 16A from HYREL 3D was used to print the electrically conductive layer using the prepared resin (see Figure 2). Hydra 16A is a large volume printer capable of printing up to 600 mm in the Z-direction. For the present work, a screw-driven 25 cc aluminum syringe (EMO-25) was utilized. The volume of the syringe was not enough to print a complete layer of 17 cm × 17 cm size in one go. When it was empty, printing was stopped, the syringe was refilled, and printing was restarted in the same location. In the future, a high-volume syringe should be used to avoid discontinuity in the print. The Hydra 16A printer is capable of printing on a heated bed using a heated nozzle, but for the current work, no extra heat was provided during printing. A 1 mm nozzle was used for the printing, as shown in Figure 3.

Figure 2. Hydra 16A printer used to print thermoset electrically conductive polymer.

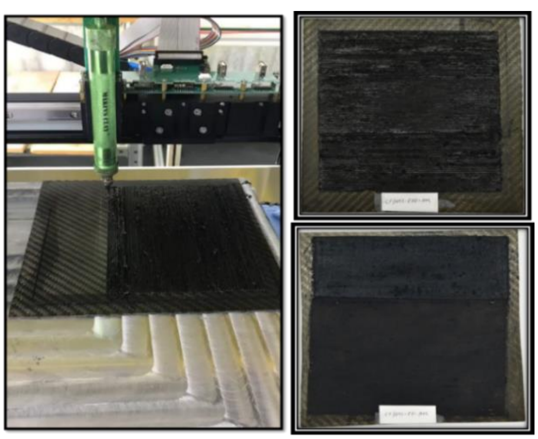

Figure 3. 3-D printing of PANI-based LSP

Lightning Strike Testing

The artificial lightning test was conducted at the NTS-Pittsfield lightning strike and protection test facility. The facility has high voltage impulse generators that can produce up to 2.4 million volts and high current-generators that can produce more than 200 kA of impulse current. This facility is also capable of producing lightning waveform components A, B, and C at the same time, but needs to perform component D separately.

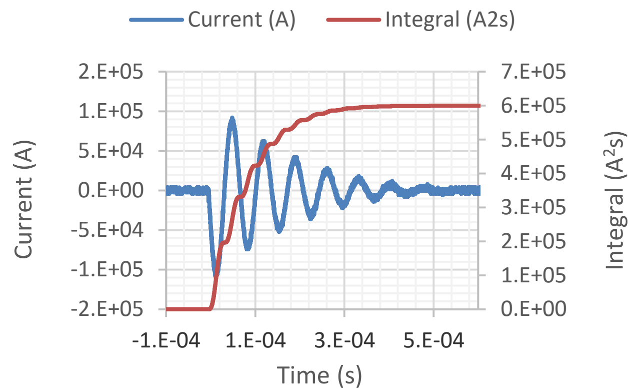

(a)

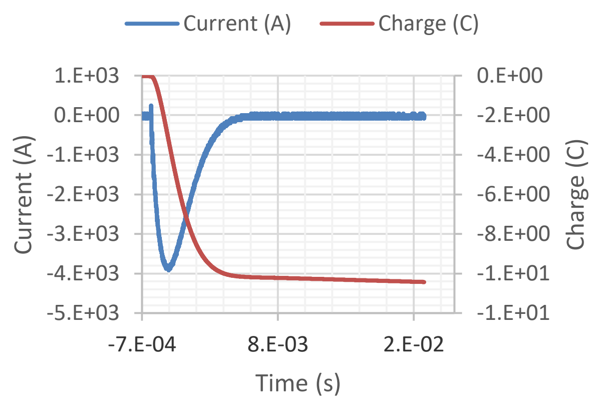

(b)

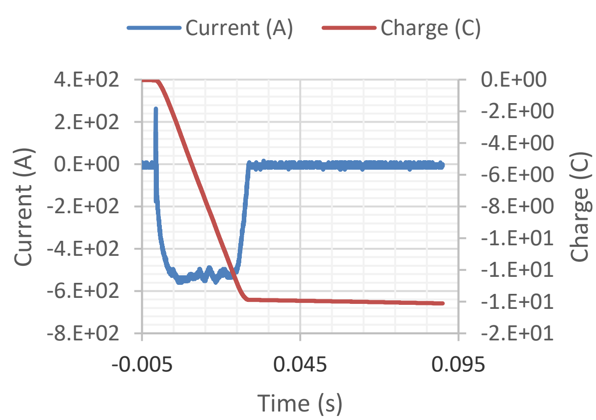

(c)

Figure 4. Applied lightning current waveform components (a) Component A, (b) Component B, and (c) Component C.

According to the SAE ARP-5412B standard for aircraft lightning environment and related test waveform, a simulated lightning strike of a continuous waveform of component A (100 kA), B (2 kA) and C (470 A) was applied [14]. The action integral and charge transfer during the lightning test were calculated as explained in ref. [15] and are shown in Table 2. The current waveforms for one of the test samples are shown in Figure 4.

The setup generator works on RLC circuits, whose values were adjusted to obtain the desired waveforms of a lightning strike. A spherical Jet diverter electrode was held 25 mm above the specimen. A small electrically conductive thread was hung from the Jet diverter towards the specimen. The specimen was placed on a wooden structure and clamped with braided aluminum bars to enable the safe transfer of current to the earthing circuit in the facility. A high-speed camera, thermal camera, and still camera were used to capture the transient lightning test. Three Tektronix oscilloscopes were employed to measure each lightning waveform component.

RESULTS

Visual Damage Analysis

Initial damage assessment was done from the images obtained via still photography and videography. A Chronos 1.4 gigapixel-per-second high-speed camera was used to capture the lightning strike events at 5100 fps. The lightning attachment on the surface of the samples and the samples after a lightning strike are shown in Figure 5. It was observed that the unprotected painted CFRP panel suffered the highest damage compared to the sample with 3D printed PANI-LSP layers. Although the PANI-layers suffered catastrophic damage to themselves, they acted as the sacrificing layer to protect the substrate CFRP structure. The damage to the printed PANI-layers can be attributed to the low adhesion bonding strength between the printed layers and the substrate structure. The mechanical load during each lightning strike that was produced from shock wave generation caused transient panel deformation, and hence the PANI layer was stripped away from the panel [16,17]. The lightning current applied in the present study was comprised of 3 components of a lightning waveform: the first return stroke, the intermediate current and the continuous current. The duration of component C lasted for a few milliseconds, and therefore it can be stipulated that once the protective layer of PANI-LSP stripped away, the lightning current was able to penetrate the CFRP panels. On the other hand, the damage to the painted panel was dominated by the dielectric behavior of the paint, which hindered a smooth and quick dissipation of the lightning current and caused more severe damage to the panels.

Another interesting observation was the different damage behavior in the CF/BMI-PD panel. With a thicker PANI-layer, the sample sustained less damage compared to the part protected by a thin PANI-LSP layer. This shows that the thickness of the electrically conductive layers also plays a vital role in suppressing lightning strike damage.

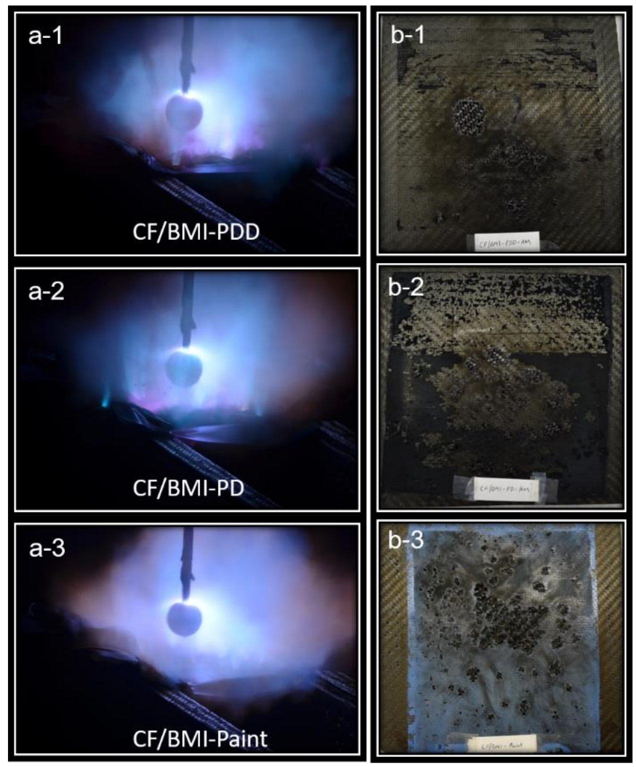

Figure 5. (a) Lightning attachment to the CFRPs (b) Samples after the lightning strike

Thermal Imaging

A FLIR T540 thermal camera was employed to capture the change in temperature on the surface of

Table 2. Artificial lightning current waveform parameters.

	Component A			Component B		Component C		
Sample	Peak Current (-kA)	Waveform *Time to peak/ Time to half* (µs)	Action Integral, *I* (A^2 s)	Average Current (-kA)	Electric charge, *Q* (-C)	Average Current (-A)	Electric charge, *Q* (-C)	Duration (ms)
CF/BMI-PDD	105	17.10/129	5.99E5	1.99	9.97	477	13.80	28.90
CF/BMI-PD	105	16.40/130	6.19E5	2.00	10.00	445	14.60	32.80
CF/BMI-Paint	105	16.40/130	6.22E5	2.01	10.00	481	13.70	28.40

the CFRP panels after lightning strikes, as shown in Figure 6. The FLIR camera used for this study had the capability to capture a maximum temperature of only 160°C, and therefore, the actual temperature change could not be observed.

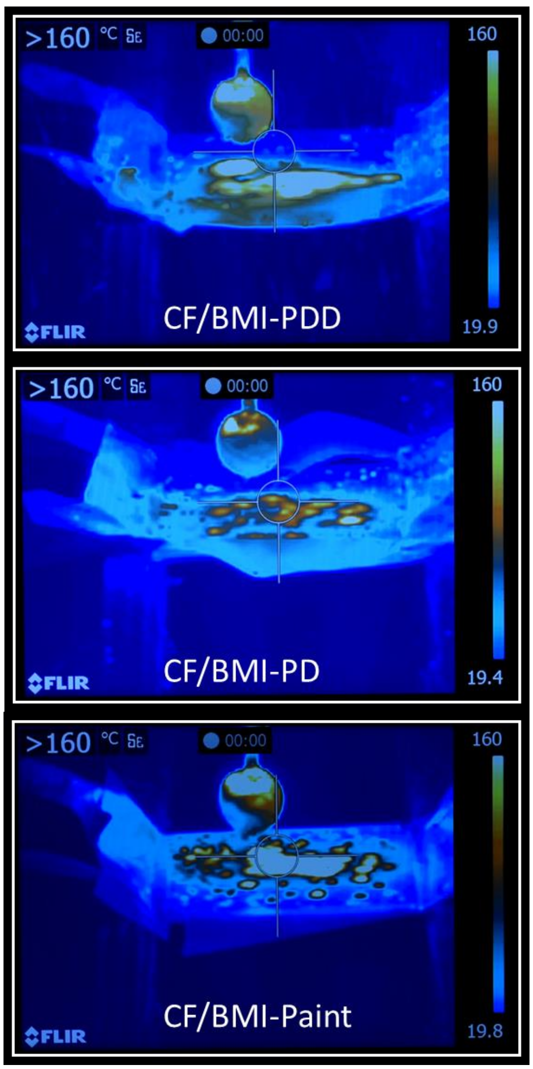

Figure 6. Thermography images after lightning strikes on the CFRP panels

On the other hand, thermal images helped understand the path taken by the lightning current from the attachment location to the grounding setup. Radiant glow on the surface of the panels could be assigned to the heat generated from the resistive heating. The thermal patches (glowing area) in the unprotected sample were scattered throughout the surface of the panel, which suggests an unavailable continuous conductive path for the lightning current to effectively dissipate.

In the case of the 3D printed PANI-LSP layer, a better dissipation of the current was observed. Damage to the CFRP panels due to Joule's heat was able to be understood through thermal imaging.

Ultrasonic Inspection:

Ultrasonic inspection was performed to qualitatively visualize the damaged locations on the surface of the composites after the lightning strike test. An Olympus OmniScan SX phased array system was used to capture inspection data. The inspection setup was a pulse-echo scan, normal to the damaged surface, within an immersion tank that produced a 1.0-mm scan resolution. The three specimens were inspected using a 64 element, linear phase array transducer (5L64-NW1) with 5 MHz frequencies. The scan parameters had an overall gain of 8 dB and a band-pass filter was applied with a center frequency of 2.3 MHz and a 1.0 – 3.5 MHz bandwidth. This allowed surface and sub-surface analyses of the damaged caused by the lightning strike.

The ultrasonic results were able to depict the damaged areas on the composite. The gate was placed at the front wall echo with the band-pass filter applied to inspect damage at the surface and sub-surface. A typical signal response of the undamaged areas on the composite produces a 60% signal amplitude (yellow) in the ultrasound C-Scan. Signatures of the lightning strike damage appear on the ultrasound C-Scan as low amplitudes, below 30% (blue), due to the scattering and absorption caused by the out-of-plane damage. It was also concluded the damage was localized at the damage sights and did not spread radially throughout the sub-surface or thickness. The damage captured by ultrasound matched well with the visual inspections for all composites and their defect dimensions.

The ultrasonic testing results were found to be in complete agreement with the thermography analysis. Scattered damages to the CFRP panel in the case of the unprotected panel are visible in Figure 7. Damages to the 3D printed PANI-layer protected samples were significantly low compared to the unprotected samples, which confirms the effectiveness of the 3D printed layers. The sample with a thicker PANI-LSP layer performed even better and showed little damage.

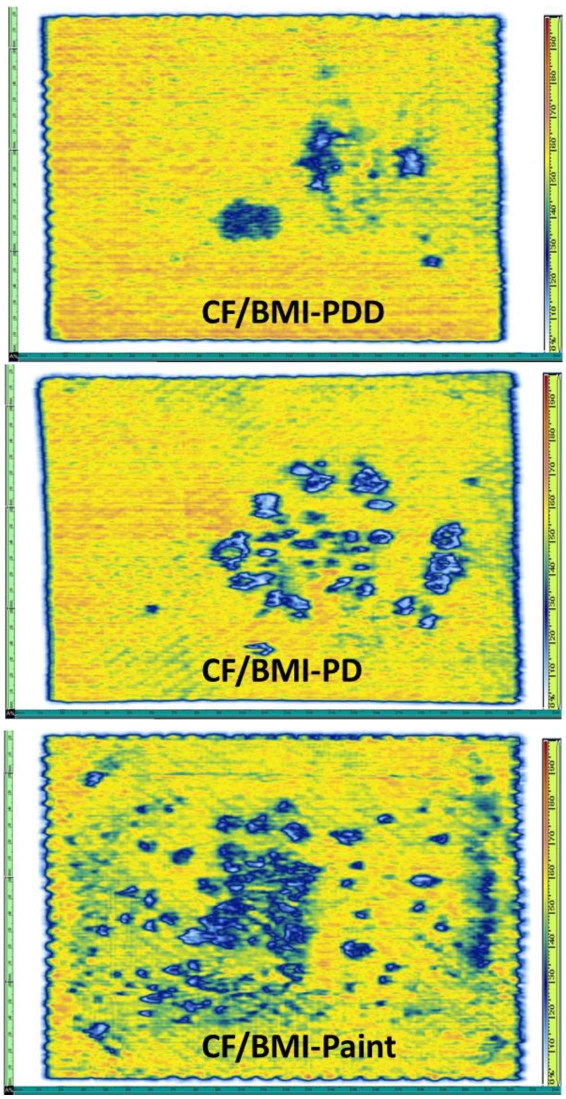

Figure 7. Ultrasonic inspection of the CFRP panels after lightning strikes.

CONCLUSION

In this work, two trending research topics, (a) lightning strike protection of CFRPs using non-metallic polymeric materials and (b) additive manufacturing in composite processing, were integrated to create a 3D printable (all-polymeric) electrically conductive layer for LSP of a CFRP substrate. A polyaniline-based thermosetting resin was chosen as the printable conductive material. A painted (unprotected) CFRP panel was also subjected to a similar lightning test for comparison. Thermography and ultrasonic inspection showed that the PANI-LSP provided a continuous conductive path to effectively dissipate the lightning current. However, the bonding strength between printed layers and substrate structure was low and needs to be improved in future work.

ACKNOWLEDGMENT

Research sponsored by the U.S. Department of Energy, Office of Energy Efficiency and Renewable Energy, Industrial Technologies Program, under contract DE-AC05-00OR22725 with UT-Battelle, LLC.

REFERENCES

[1] H.L. Tekinalp, V. Kunc, G.M. Velez-Garcia, C.E. Duty, L.J. Love, A.K. Naskar, C.A. Blue, S. Ozcan, Highly oriented carbon fiber-polymer composites via additive manufacturing, Compos. Sci. Technol. 105 (2014) 144–150. doi:10.1016/j.compscitech.2014.10.009.

[2] T. Smith, J. Failla, J. Lindahl, S. Kim, A.A. Hassen, C. Duty, P. Joshi, C. Stevens, V. Kunc, Structural Health Monitoring of 3D Printed Structures, (2018) 2211–2218.

[3] V. Kunc, A.A. Hassen, J. Lindahl, S. Kim, B. Post, LARGE SCALE ADDITIVELY MANUFACTURED, (2017).

[4] T.D. Ngo, A. Kashani, G. Imbalzano, K.T.Q. Nguyen, D. Hui, Additive manufacturing (3D printing): A review of materials, methods, applications and challenges, Compos. Part B Eng. 143 (2018) 172–196. doi:10.1016/j.compositesb.2018.02.012.

[5] C. Ajinjeru, V. Kishore, J. Lindahl, Z. Sudbury, A.A. Hassen, B. Post, L. Love, V. Kunc, C. Duty, The influence of dynamic rheological properties on carbon fiber-reinforced polyetherimide for large-scale extrusion-based additive manufacturing, (2018).

[6] D. Jiang, D.E. Smith, Mechanical Behavior of Carbon Fiber Composites Produced with Fused Filament Fabrication, 27th Annu. Int. Solid Free. Fabr. Symp. (2016) 884–898. doi:10.1016/j.addma.2017.08.006.
[7] C. Karch, C. Metzner, Lightning protection of carbon fibre reinforced plastics - An Overview, 2016 33rd Int. Conf. Light. Prot. ICLP 2016. (2016). doi:10.1109/ICLP.2016.7791441.
[8] V. Kumar, S. Sharma, A. Pathak, B.P. Singh, S.R. Dhakate, T. Yokozeki, T. Okada, T. Ogasawara, Interleaved MWCNT buckypaper between CFRP laminates to improve through-thickness electrical conductivity and reducing lightning strike damage, Compos. Struct. (2019). doi:10.1016/j.compstruct.2018.11.088.
[9] V. Kumar, T. Yokozeki, T. Okada, Y. Hirano, T. Goto, T. Takahashi, A.A. Hassen, T. Ogasawara, Polyaniline-based all-polymeric adhesive layer: An effective lightning strike protection technology for high residual mechanical strength of CFRPs ☆, (2019). doi:10.1016/j.compscitech.2019.01.006.
[10] V. Kumar, T. Yokozeki, T. Okada, Y. Hirano, T. Goto, T. Takahashi, T. Ogasawara, Effect of through-thickness electrical conductivity of CFRPs on lightning strike damages, Compos. Part A Appl. Sci. Manuf. 114 (2018) 429–438. doi:10.1016/J.COMPOSITESA.2018.09.007.
[11] A. Katunin, K. Krukiewicz, R. Turczyn, P. Sul, K. Dragan, Lightning strike resistance of an electrically conductive CFRP with a CSA-doped PANI/epoxy matrix, Compos. Struct. 181 (2017) 203–213. doi:10.1016/j.compstruct.2017.08.091.
[12] Y. Hirano, T. Yokozeki, Y. Ishida, T. Goto, T. Takahashi, D. Qian, S. Ito, T. Ogasawara, M. Ishibashi, Lightning damage suppression in a carbon fiber-reinforced polymer with a polyaniline-based conductive thermoset matrix, Compos. Sci. Technol. 127 (2016) 1–7. doi:10.1016/j.compscitech.2016.02.022.
[13] A.K. Pathak, M. Borah, A. Gupta, T. Yokozeki, S.R. Dhakate, Improved mechanical properties of carbon fiber/graphene oxide-epoxy hybrid composites, Compos. Sci. Technol. 135 (2016) 28–38. doi:10.1016/j.compscitech.2016.09.007.
[14] SAE ARP 5412A, Aircraft lightning environment and related test waveforms, 2005.
[15] V. Kumar, T. Yokozeki, T. Okada, Y. Hirano, T. Goto, T. Takahashi, T. Ogasawara, Effect of through-thickness electrical conductivity of CFRPs on lightning strike damages, Compos. Part A Appl. Sci. Manuf. 114 (2018) 429–438. doi:10.1016/j.compositesa.2018.09.007.
[16] C. Karch, M. Schreiner, Shock Waves from a Lightning Discharge, (2018). doi:10.1109/ICLP.2018.8503327.
[17] C. Karch, A. Arteiro, P.P. Camanho, Modelling mechanical lightning loads in carbon fibre-reinforced polymers, Int. J. Solids Struct. 162 (2018) 217–243. doi:10.1016/j.ijsolstr.2018.12.013.